Controlled AFM manipulation of small nanoparticles and assembly of hybrid nanostructures

2011 Nanotechnology 22 115301

(http://iopscience.iop.org/0957-4484/22/11/115301)

Nanotechnology **22** (2011) 115301 (6pp) doi:10.1088/0957-4484/22/11/115301

Controlled AFM manipulation of small nanoparticles and assembly of hybrid nanostructures

Suenne Kim, Farbod Shafiei, Daniel Ratchford and Xiaoqin Li

Department of Physics, Center for Nano- and Molecular Science and Technology, University of Texas at Austin, Austin, TX 78712, USA

E-mail: elaineli@physics.utexas.edu

Received 6 September 2010, in final form 25 November 2010
Published 8 February 2011
Online at stacks.iop.org/Nano/22/115301

Abstract

We demonstrate controlled manipulation of semiconductor and metallic nanoparticles (NPs) with 5–15 nm diameters and assemble these NPs into hybrid structures. The manipulation is accomplished under ambient environment using a commercial atomic force microscope (AFM). There are particular difficulties associated with manipulating NPs this small. In addition to spatial drift, the shape of an asymmetric AFM tip has to be taken into account in order to understand the intended and actual manipulation results. Furthermore, small NPs often attach to the tip via electrostatic interaction and modify the effective tip shape. We suggest a method for detaching the NPs by performing a pseudo-manipulation step. Finally, we show by example the ability to assemble these small NPs into prototypical hybrid nanostructures with well-defined composition and geometry.

(Some figures in this article are in colour only in the electronic version)

1. Introduction

Currently, a major field in photonics is the study of how surface plasmon resonances of metallic NPs shape optical fields at the nanoscale [1, 2]. In hybrid photonic devices, metallic nanostructures are often used as optical antennas, cavities or waveguides which then interact with active semiconductor components [3, 4]. The interaction between the metallic and semiconductor components strongly depends on their size, shape and geometric arrangement. This feature provides great flexibility in designing custom nanophotonic devices with desired properties but also presents serious challenges in their synthesis and characterization. Many appealing hybrid nanostructures are synthesized in solution. A common problem with chemically synthesized hybrid structures is that a broad range of structures with ill-controlled configurations are produced [5, 6]. In order to reveal the intrinsic properties of hybrid nanostructures, a method for producing well-controlled prototypical hybrid nanostructures is highly desirable. Nanomanipulation methods based on micromanipulators and scanning probe microscopy are well suited for this task.

The impressive capability of manipulating individual atoms on surfaces has been previously demonstrated [7–12]. Manipulating objects with diameters ranging from a few nanometers to tens of nanometers in ambient environments, however, poses its own challenges and has broad applications in nanotechnology. AFM is particularly suitable for nanomanipulation tasks, and much progress has been made in the last decade in the area of AFM nanomanipulation. For example, nanosized objects of various shapes (e.g. spheres, rods, wires and tubes) have been manipulated on a flat substrate [13–23]. Simple three-dimensional manipulations, such as pushing an NP across a step or over other particles, have also been demonstrated [24, 13]. Automatic manipulation protocols have been devised and implemented with some success [13]. However, manipulating nano-objects with high success rates and accuracy remains challenging due to a lack of predictive understanding of adhesion and friction on the nanoscale [25–27].

In this paper, we discuss AFM nanomanipulation of colloidal CdSe/ZnS semiconductor NPs with 5–8 nm diameters and colloidal Au metallic NPs with 15 nm diameters. While standard AFM nanomanipulation works well for relatively

large NPs, manipulating NPs smaller than the size of the AFM probe apex remains challenging. In what follows, we review several important technical aspects in manipulating small NPs. First, a system with excellent mechanical/thermal stability is critical for successful manipulation of small NPs. Second, the asymmetric shape of the tip must be taken into account in order to understand the intended and actual manipulation results. Third, small NPs often adhere to the tip and lead to a modified effective tip shape. We suggest a method for detaching the NP by performing a pseudo-manipulation step. Finally, we present an example of an assembled hybrid nanostructure in which four Au NPs surround one CdSe/ZnS NP in a well-defined geometry. Although the components of such a hybrid structure are not physically linked (e.g. by molecules), their properties still change because of photonic and electronic interactions among the components. For example, the photoluminescence lifetime of the semiconductor emitter may shorten due to both the modified electromagnetic environment and the non-radiative energy transfer to the metallic NPs.

2. Method

We use a standard protocol that has been previously applied for nanomanipulation. The manipulation process consists of several steps as illustrated in figure 1. NPs are first imaged with the feedback engaged, as shown in figure 1(a), and an NP is selected to be manipulated. Next, using commercial manipulation software, a line is drawn that starts behind the chosen NP and ends at the target position (figure 1(b)). The tip is then positioned behind the NP. The tip moves along the trajectory defined by the line on the screen (figure 1(c)) and pushes the NP upon contact. In this pushing step, the z feedback is disengaged. Once the tip reaches the target position, the AFM probe is pulled away and the feedback is re-engaged. Finally, the sample is imaged again to examine the result of the manipulation. If the NP is not at the target position, this multi-step procedure is repeated. An interesting question to ask is how NPs (especially spherical and cylindrical NPs) move on the substrate during the manipulation, i.e. do they slide or roll? This question is debated in the literature [28, 29]. No general rules are currently known. The experiments presented here do not address this particular question.

A closed-loop commercial AFM (Veeco-Dimension 3100) operated under ambient environment was used for nanomanipulation. The NanoMan software from Veeco was employed, which compensates for hysteresis and drift to some degree. Soft tapping mode cantilevers from Mikromasch were used with nominal force constants of ∼5–7.5 N m^{-1}. Samples were prepared on quartz substrates (Meller Optics) with a surface roughness of ∼2 nm. The substrates were cleaned with a solution of sulfuric acid (H_2SO_4, 98%) and hydrogen peroxide (H_2O_2, 30%) mixed with a ratio of 1:1, rinsed with deionized water and then dried with high purity nitrogen gas. Colloidal Au NPs with nominally 15 nm diameter (British Biocell, 15704-20) were suspended in water at a concentration of 1.4×10^{12} particles ml^{-1}. CdSe/ZnS core/shell NPs (NN-labs, CZ620-25, ∼5 nm diameters) with an original concentration of 1.6×10^{-5} mol l^{-1} were diluted with toluene to 10^{-9} mol l^{-1}. The NPs were spin-coated at 4000 rpm onto the substrates, and then the substrates were heated at 100 °C for a few minutes to dry. Typical AFM parameters used for manipulating the small NPs are the following: a low integrative gain of ∼0.15, a proportional gain ∼0.3 and a scanning speed of 1 μm s^{-1} for imaging and 5–20 μm s^{-1} for manipulation. The scanning area was typically limited to ∼1 μm × 1 μm to avoid the bowing effect. Z offset relative to the substrate is typically from −10 to 20 nm for cantilevers with a large spring constant (20 N m^{-1} or larger). For cantilevers with a small spring constant (5 N m^{-1}), Z offset is typically set from −40 to −20 nm.

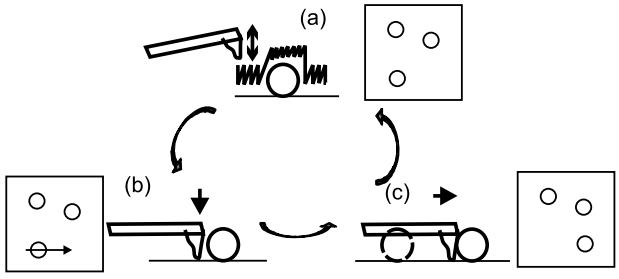

Figure 1. Schematics of the manipulation method. (a) First, an image is taken. (b) The tip is positioned behind the NP to be manipulated and a line is drawn using commercial software. (c) The tip pushes the NP in contact mode. Another image is taken to examine the result of manipulation. If the NP did not move to the target position, the process is repeated.

3. Results and discussion

It is challenging to manipulate a NP with a small diameter, especially when moving the NP over longer distances [13]. If a particle is not struck directly at its center, the particle may slip away from the tip and the manipulation fails [13]. It takes 5–10 min to scan a 1 μm × 1 μm area to obtain clear images of small NPs. Spatial drift as small as a few nanometers during this time may be problematic for the following manipulation step. A system with excellent mechanical stability is clearly a prerequisite for successful nanomanipulation. Nevertheless, spatial uncertainties originating from thermal drift or nonlinearities of piezo actuators, such as hysteresis and creep, cannot be eliminated completely. Before any manipulation, a few images should be taken to examine the degree and direction of spatial drift between the sequential images. User correction is often necessary by anticipating the NPs' locations, taking into account the drift. A different manipulation method based on sweeping NPs is less susceptible to spatial drift but is more difficult to control the precise direction of NP motion [30, 31].

The shape of an asymmetric tip plays a significant role in predicting the motion of the NP during manipulation. AFM images (figure 2) taken before and after manipulating an NP in two opposite directions demonstrate this AFM probe-shape-dependent effect clearly. To move a 15 nm NP to the right, the arrow was created to direct the tip motion as shown in figure 2(a). The image taken after the manipulation

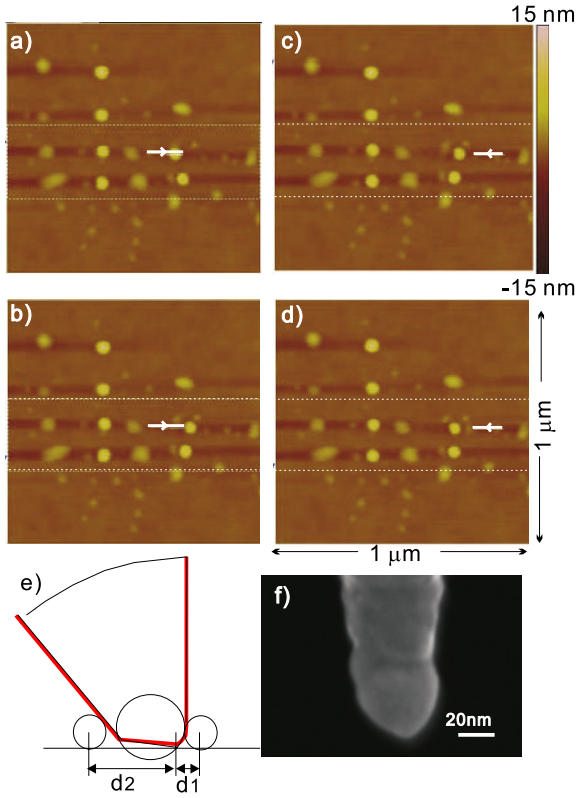

Figure 2. Illustration of the tip-asymmetry effect using Au NPs with 15 nm diameters. The images before (a) and after (b) a manipulation step in which the NP is pushed to the right. The images before (c) and after (d) a manipulation step in which the NP is pushed to the left. Only areas between dotted lines are updated following the manipulation. Although the arrow in (c) did not appear to touch the NP on the screen, the NP moved in (d). (e) A schematic of an asymmetric tip. The sphere at the end of the tip represents a perfectly symmetric tip and the red line outlines an asymmetric shape resulting from the manufacturing process or abrasion during manipulation. (f) An SEM image of a typical AFM tip exhibits the asymmetric shape.

(figure 2(b)) shows the NP was moved successfully to the target position at the end of the arrow. We then attempted to move the NP to the left by drawing the cursor shown in figure 2(c). Since the arrow is placed some distance away from the NP, visually the NP might be expected to stay in its original position. The particle, however, moved to the left as shown in figure 2(d). One obvious reason that may cause such a directional asymmetry in manipulation is spatial drift. However, the spatial drift (∼10 nm) between subsequent images alone cannot explain the separation between the tip and the end of the arrow (∼40 nm) in this case. The difference between manipulations in opposite directions can also be caused by the asymmetric tip shape resulting from tip manufacturing, mounting processes and/or abrasion. As illustrated in the schematic in figure 2(e), the distances between the center of the NP and the apex of the tip are different, depending on whether the NP is positioned to the left or right side of the tip. In moving the NP to the right, the tip starts to push the NP at a distance of d_1. In moving the NP to the left, however, the tip starts to push the NP at a distance of d_2. Because d_2 is larger than d_1, the NP moved to the left in figure 2(d) even though the arrow did not appear to contact the NP. In the schematics shown in figure 2(e), the ratio between the diameter of the tip and NP is 2:1. If the diameter of the NP is taken as 15 nm, the difference between d_2 and d_1 is more than 25 nm. This tip shape effect is always present. The effect, however, is especially visually striking for this particular combination of particle size and tip shape. Shown in figure 2(f) is a scanning electron microscope (SEM) image (taken by a Hitachi S-5500) of a typical tip (Mikromasch, NSC-35-B) in which the asymmetric tip shape is clearly visible. Because of the large variation in tip shapes, we suggest the user to always gauge the asymmetric tip shape by performing test manipulations in all four directions (up, down, left and right). The difference between the apparent arrow positions and final NP positions depends on the direction of manipulation and must be taken into account for precisely placing a small NP at a target position.

Small metallic or semiconductor NPs often adhere to the tip via electrostatic interaction during nanomanipulation. There are two signatures for this sticking event: the NP is missing in the next image and the spatial resolution of the image might change due to the modified 'effective tip shape'. In the example shown in figure 3, we used Au NPs with diameters ranging from 8 to 15 nm and an AFM tip with a radius of curvature of 15–20 nm. For the purpose of nanomanipulation, attached NPs need to be dropped before the next manipulation step. One method for detaching the NP is to perform a 'pseudo'-manipulation step, as illustrated in figure 3. An AFM image was taken and the NP enclosed in the box was chosen to be manipulated (figure 3(a)). An arrow was created to direct the tip motion (white arrow in figure 3(b)) and the resulting AFM image after the tip motion is shown in figure 3(b). Only the portion of the image between the two dashed lines was updated. Notice the selected NP is missing from the AFM image and the spatial resolution in the updated area was different from the rest of the image in figure 3(b). These changes suggest the NP is attached to the tip and the convoluted spatial resolution in the updated region was determined by the modified tip rather than the bare tip[1]. To drop the NP, we chose a clean area on the substrate and drew an arrow away from the NP as shown in figure 3(c). The whole area was rescanned following the pseudo-manipulation step and all the NPs between the two dotted lines in figure 3(b) now look larger compared to those in the same region in figure 3(b). The detached NP (enclosed in the box) left behind can also be observed. We note that there are additional small surface features in figure 3(c) along the path of the manipulation highlighted in figure 3(b). These small features are residues from the Au NP. We observe such residues left from Au NPs in many cases.

The drop-off method described above is based on the fact that the adhesion force is a function of time. As the contact time between two surfaces increases, the adhesion force increase. Schematics illustrating the process of attachment and

[1] These images are captured real-time screen displays. The image in figure 3(b) is not taken immediately following figure 3(a). We did not display an intermediate manipulation step. In addition, we note that some spatial drift has occurred.

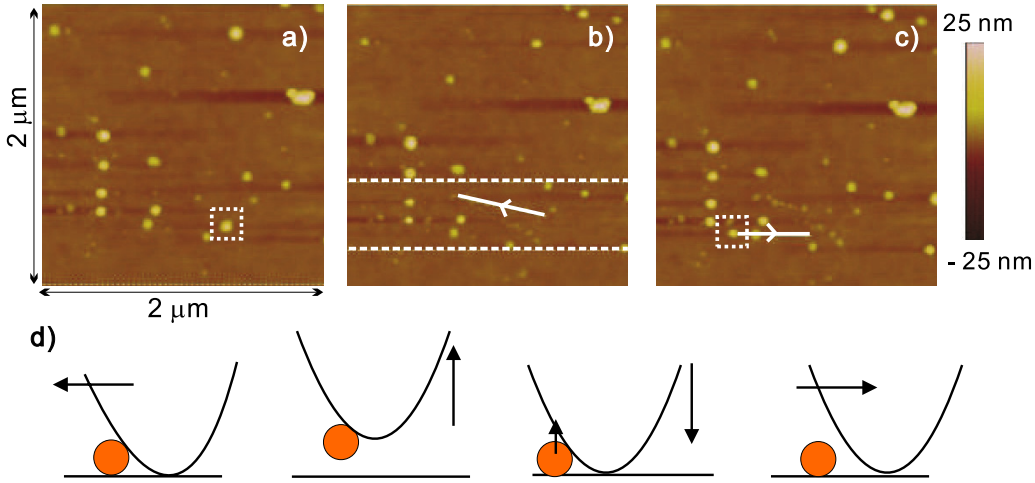

Figure 3. A method for dropping an NP demonstrated with Au NPs with 15 nm diameter. (a) An image taken before any manipulation and the NP enclosed in the box was chosen to be manipulated. (b) Real-time image in which the area between two dotted lines was updated after manipulation. The chosen NP went missing. The spatial resolution was slightly improved. (c) A pseudo-manipulation step in which the NP enclosed in the box was dropped at the beginning of the line. (d) Schematics of picking up and dropping off a NP. The attached NP was disturbed in the pseudo-manipulation step, the adhesion force was reduced, and the NP dropped when the tip was drawn away.

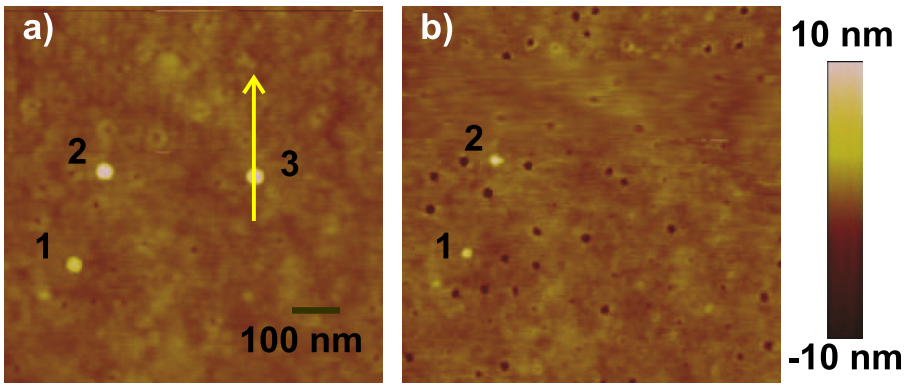

Figure 4. Improved spatial resolution after a small NP (CdSe/ZnS core/shell NPs with ∼5 nm diameter) is attached near the apex of the AFM probe. (a) An image taken before any manipulation. The manipulation step is defined by the yellow arrow. (b) An image taken after the manipulation step. NP 3 was picked up and adhered near the apex of the tip.

the following detachment are shown in figure 3(d). In the first step, the tip pushes the NP to the left and the NP attaches to the tip. Next, by pressing the tip down, the NP is perturbed and the adhesion force between the NP and tip is reduced. If the tip is dragged away immediately, there is a high possibility to detach the NP. We have prepared ten different batches of samples (Au NPs on quartz, glass and Si). For each batch of sample, 50 manipulations were performed on average. Au NPs stuck on the tip during ∼30% of the manipulations. All NPs were dropped with 1–2 pseudo-manipulation steps[2]. We note that this drop-off method was used to detach carbon nanotubes from an AFM tip with a similar success rate.

When manipulating very small NPs, the NP may attach very close to the tip of the AFM probe and lead to an improved spatial resolution in the subsequent images. We present one such example of manipulating CdSe/ZnS NPs (∼5 nm diameter). After taking an initial image of sparsely dispersed CdSe/ZnS NPs, a manipulation step was attempted as indicated by the arrow in figure 4(a). Following this manipulation, another image (figure 4(b)) was taken to examine the result. The chosen NP (particle 3) was not present in the second scan. In addition, the resolution of the image clearly improved, indicating that the 5 nm NP was attached to the AFM tip. In certain applications, it may be desirable to attach an NP to the tip. Similar modified probes have been used to improve optical imaging [32] and conduct measurements of single-nanoparticle interactions [33], resonant energy transfer [34], adhesive forces [35] and scattering [36]. In order to achieve this goal, one can use a probe with a low aspect ratio, bring the probe lower to increase the contact area between the probe and NP, and push the NP at a slow scan speed to increase the contact time.

Finally, we present an example of a hybrid nanostructure consisting of four 15 nm Au NPs and one 5 nm CdSe/ZnS NP. The samples were diluted and spin-coated in such a way as to obtain a few NPs in a 2 μm × 2 μm area (figure 5(a)).

[2] An NP attached to the tip may also become detached when one tries to manipulate another NP. In this case, one may have to try manipulating the second NP in different directions before the first attached NP is perturbed and falls off.

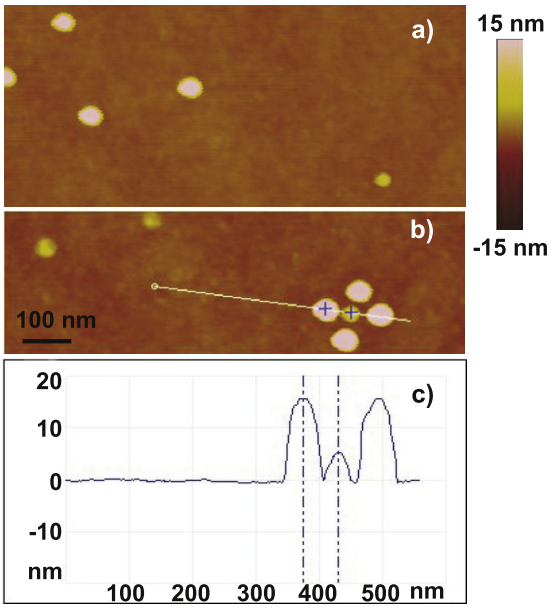

Figure 5. An example of an assembled hybrid structure consisting of Au NPs (∼15 nm diameter) and CdSe/ZnS core/shell NPs (∼5 nm diameter). (a) An image before any manipulation. (b) The assembled hybrid structure where a CdSe/ZnS NP is surrounded by four Au NPs. (c) A line cut shown in (b).

Both the semiconductor and metallic NPs were manipulated in multiple steps. In particular, Au NPs were moved up to 2 μm. By design, each Au NP should be a distance of 55 nm from the CdSe/ZnS NP. Through inspection of multiple cross sections of the AFM scan shown in figures 5(b) and (c), we measured the distances between Au and CdSe/ZnS NPs to be 54.2 ± -1.1 nm, 52.8 ± -0.8 nm, 61.8 ± -1.1 nm and 59.0 ± -1.0 nm in the clockwise direction starting from the Au NP on the left. Two small surface features appear in the upper left corner of figure 5(b). Again, they are due to residues of Au NPs that have been pushed away. Photonic properties of hybrid structures strongly depend on the size, shape and geometric arrangement of the components. The nanomanipulation method is a suitable method for assembling such structures as demonstrated in this example.

4. Conclusion

We have demonstrated the assembly of hybrid nanostructures under ambient conditions using a commercial AFM and its control software. Although the manipulation method has been applied previously, we discussed a few technical issues that help to improve the success rate and accuracy of manipulating NPs with diameters of 15 nm or smaller. In additional to spatial drift, an asymmetric tip may cause the NP to end up in a different position from the end of the arrow. The deviation depends on the specific direction of manipulation. Users are advised to gauge the tip shape by performing test manipulation steps in different directions and to adjust the manipulation accordingly for precise placement of the NP. In the event that a small NP unintentionally attaches to the tip, one can drop the NP by performing a pseudo-manipulation step. This drop-off method takes advantage of the time-dependent nature of adhesion and has been shown to work with a high success rate. Finally, we demonstrated that one can assemble hybrid nanostructures with well-controlled compositions and geometries. Future experiments capable of providing simultaneous structural and optical/electrical characterizations on individual nanostructures will help reveal their intrinsic properties and promote the development of nanophotonic devices based on hybrid materials.

Acknowledgments

We gratefully acknowledge financial support from the following sources: NSF DMR-0747822, ONR N00014-08-1-0745, AFOSR-FA9550-10-1-0022, Welch Foundation F-1662 and the Alfred P Sloan Foundation. DR acknowledges a fellowship from the NSF-IGERT program via grant DGE-0549417.

References

[1] Barnes W L, Dereux A and Ebbesen T W 2003 Surface plasmon subwavelength optics *Nature* **424** 824–30
[2] Pelton M, Aizpurua J and Bryant G 2008 Metal-nanoparticle plasmonics *Laser Photon. Rev.* **2** 136–59
[3] Bozhevolnyi S I, Volkov V S, Devaux E, Laluet J Y and Ebbesen T W 2006 Channel plasmon subwavelength waveguide components including interferometers and ring resonators *Nature* **440** 508–11
[4] Muhlschlegel P, Eisler H J, Martin O J F, Hecht B and Pohl D W 2005 Resonant optical antennas *Science* **308** 1607–9
[5] Prabhu V M and Hudson S D 2009 Nanoparticle assembly: DNA provides control *Nat. Mater.* **8** 365–6
[6] Chen W, Bian A, Agarwal A, Liu L, Shen H, Wang L, Xu C and Kotov N A 2009 Nanoparticle superstructures made by polymerase chain reaction: collective interactions of nanoparticles and a new principle for chiral materials *Nano Lett.* **9** 2153–9
[7] Stroscio J A and Eigler D M 1991 Atomic and molecular manipulation with the scanning tunneling microscope *Science* **254** 1319–26
[8] Eigler D M and Schweizer E K 1990 Positioning single atoms with a scanning tunnelling microscope *Nature* **344** 524–6
[9] Manoharan H C, Lutz C P and Eigler D M 2000 Quantum mirages formed by coherent projection of electronic structure *Nature* **403** 512–5
[10] Sugimoto Y, Abe M, Hirayama S, Oyabu N, Custance O and Morita S 2005 Atom inlays performed at room temperature using atomic force microscopy *Nat. Mater.* **4** 156–9
[11] Sugimoto Y, Pou P, Custance O, Jelinek P, Abe M, Perez R and Morita S 2008 Complex patterning by vertical interchange atom manipulation using atomic force microscopy *Science* **322** 413–7
[12] Oyabu N, Custance Ó, Yi I, Sugawara Y and Morita S 2003 Mechanical vertical manipulation of selected single atoms by soft nanoindentation using near contact atomic force microscopy *Phys. Rev. Lett.* **90** 176102
[13] Requicha A A G 2008 *Nanotechnology* ed R Waser (Weinheim: Wiley–VCH) pp 239–73
[14] Ramachandran T R, Baur C, Bugacov A, Madhukar A, Koel B E, Requicha A and Gazen C 1998 Direct and controlled manipulation of nanometer-sized particles using the non-contact atomic force microscope *Nanotechnology* **9** 237–45

[15] Kim Y and Lieber C M 1992 Machining oxide thin films with an atomic force microscope: pattern and object formation on the nanometer scale *Science* **257** 375–7
[16] Luthi R, Meyer E, Haefke H, Howald L, Gutmannsbauer W and Guntherodt H J 1994 Sled-type motion on the nanometer scale: determination of dissipation and cohesive energies of C60 *Science* **266** 1979–81
[17] Schaefer D M, Reifenberger R, Patil A and Andres R P 1995 Fabrication of two-dimensional arrays of nanometer-size clusters with the atomic force microscope *Appl. Phys. Lett.* **66** 1012–4
[18] Hertel T, Martel R and Avouris P 1998 Manipulation of individual carbon nanotubes and their interaction with surfaces *J. Phy. Chem.* B **102** 910–5
[19] Decossas S, Mazen F, Baron T, Brémond G and Souifi A 2003 Atomic force microscopy nanomanipulation of silicon nanocrystals for nanodevice fabrication *Nanotechnology* **14** 1272–8
[20] Hsieh S, Meltzer S, Wang C R C, Requicha A A G, Thompson M E and Koel B E 2002 Imaging and manipulation of gold nanorods with an atomic force microscope *J. Phys. Chem.* B **106** 231–4
[21] Chen H, Xi N and Li G 2006 CAD-guided automated nanoassembly using atomic force microscopy-based nonrobotics *IEEE Trans. ASE* **3** 208–17
[22] Junno T, Deppert K, Montelius L and Samuelson L 1995 Controlled manipulation of nanoparticles with an atomic force microscope *Appl. Phys. Lett.* **66** 3627–9
[23] Gnecco E, Rao A, Mougin K, Chandrasekar G and Meyer E 2010 Controlled manipulation of rigid nanorods by atomic force microscopy *Nanotechnology* **21** 215702
[24] Baur C, Bugacov A, Koel B E, Madhukar A, Montoya N, Ramachandran T R, Requicha A A G, Resch R and Will P 1998 Nanoparticle manipulation by mechanical pushing: underlying phenomena and real-time monitoring *Nanotechnology* **9** 360–4
[25] Schirmeisen A and Schwarz U D 2009 Measuring the friction of nanoparticles: a new route towards a better understanding of nanoscale friction *Chem. Phys. Chem.* **10** 2373
[26] Rao A, Wille M L, Gnecco E, Mougin K and Meyer E 2009 Trajectory fluctuations accompanying the manipulation of spherical nanoparticles *Phys. Rev.* B **80** 193405
[27] Dietzel D, Monninghoff T, Herding C, Feldmann M, Fuchs H, Stegemann B, Ritter C, Schwarz U D and Schirmeisen A 2010 Frictional duality of metallic nanoparticles: influence of particle morphology, orientation, and air exposure *Phys. Rev.* B **82** 035401
[28] Ritter C, Heyde M, Schwarz U D and Rademann K 2002 Controlled translational manipulation of small latex spheres by dynamic force microscopy *Langmuir* **18** 7798–803
[29] Liu Z, Li Z, Wei G, Song Y, Wang L and Sun L 2006 Manipulation, dissection, and lithography using modified tapping mode atomic force microscope *Microsc. Res. Tech.* **69** 998–1004
[30] Rao A, Gnecco E, Marchetto D, Mougin K, Schonenberger M, Valeri S and Meyer E 2009 The analytical relations between particles and probe trajectories in atomic force microscope nanomanipulation *Nanotechnology* **20** 115706
[31] Kim S, Ratchford D C and Li X Q 2009 Atomic force microscope nanomanipulation with simultaneous visual guidance *ACS Nano* **3** 2989–94
[32] Ebenstein Y, Yoskovitz E, Costi R, Aharoni A and Banin U 2006 Interaction of scanning probes with semiconductor nanocrystals; physical mechanism and basis for near-field optical imaging *J. Phys. Chem.* A **110** 8297–303
[33] Vakarelski I U and Higashitani K 2006 Single-nanoparticle-terminated tips for scanning probe microscopy *Langmuir* **22** 2931–4
[34] Ebenstein Y, Mokari T and Banin U 2004 Quantum-dot-functionalized scanning probes for fluorescence-energy-transfer-based microscopy *J. Phys. Chem.* B **108** 93–9
[35] Xing M, Zhong W, Xu X and Thomson D 2010 Adhesion force studies of nanofibers and nanoparticles *Langmuir* **26** 11809–14
[36] Wenzel M T, Hartling T, Olk P, Kehr S C, Grafstrom S, Winnerl S, Helm M and Eng L M 2008 Gold nanoparticle tips for optical field confinement in infrared scattering near-field optical microscopy *Opt. Express* **16** 12302–12